

Article

# The maximum wind energy of the most correlated points in an urban environment

George Efthimiou

Chemical Process and Energy Resources Institute, Centre for Research and Technology Hellas, Thessaloniki 57001, Greece;  
[gefthymiou@certh.gr](mailto:gefthymiou@certh.gr)

## CITATION

Efthimiou G. The maximum wind energy of the most correlated points in an urban environment. *Energy Storage and Conversion*. 2025; 3(2): 2211.  
<https://doi.org/10.59400/esc2211>

## ARTICLE INFO

Received: 4 December 2024  
Accepted: 8 January 2025  
Available online: 1 April 2025

## COPYRIGHT



Copyright © 2025 by author(s).  
*Energy Storage and Conversion* is published by Academic Publishing Pte. Ltd. This work is licensed under the Creative Commons Attribution (CC BY) license.  
<https://creativecommons.org/licenses/by/4.0/>

**Abstract:** This study investigates the maximum wind energy potential of points that exhibit the highest correlation in an urban environment. A wind tunnel experiment that was simulated in a previous study using the Large Eddy Simulation (LES) methodology to generate wind speed time series at various locations within a complex urban setting. The analysis focuses on the correlation of wind speeds at different heights and spatial points, demonstrating a clear dependence on height, with maximum correlations generally increasing as height increases. This phenomenon is attributed to the disruption of turbulent eddies by buildings, which significantly influences the wind flow patterns. The Spectral Proper Orthogonal Decomposition (SPOD) technique is employed to calculate the maximum wind energy, revealing that the maximum values occur on building rooftops. Additionally, an empirical equation is proposed, relating the maximum wind energy to the distance between the most correlated points, with a relatively high correlation coefficient. The findings of this research have practical implications for the optimization of renewable energy resources, particularly in urban environments where wind flow is highly complex. This study contributes to the understanding of wind energy potential in urban settings, offering insights that could be valuable for the placement and design of wind turbines in such challenging environments. The study revealed a significant dependence of wind energy potential on spatial positioning and height, with maximum values occurring at rooftops. An empirical equation was developed to predict the difference in maximum wind energy based on the distance between highly correlated points, offering a practical tool for urban wind energy optimization. These findings provide actionable insights for the integration of renewable energy systems in complex urban settings.

**Keywords:** urban wind energy; large eddy simulation (LES); wind flow correlation; spectral proper orthogonal decomposition (SPOD); renewable energy in urban environments; wind energy optimization

## 1. Introduction

The growing global demand for renewable energy sources, driven by the need to reduce greenhouse gas emissions and combat climate change, has highlighted wind energy as a key player in the transition to sustainable energy systems [1]. Wind energy is recognized as one of the most promising and scalable renewable technologies, particularly in urban environments where space is limited and energy demand is concentrated [2]. Urban wind energy, however, presents unique challenges due to the highly turbulent nature of airflow within cities, influenced by the presence of buildings and other structures [3].

Urban environments create complex wind patterns characterized by the disruption of natural airflow, leading to increased turbulence, flow separation, and

wake effects [4]. These phenomena significantly impact the performance and efficiency of wind turbines, making the optimization of their placement and design critical [5]. The interaction between wind turbines and urban structures has been the subject of numerous studies, particularly regarding the spatial correlation of wind speeds and the potential for energy capture in dense urban settings [6].

Recent research in the field has demonstrated that the spatial correlation of wind speeds plays a crucial role in optimizing turbine placement, especially in areas with significant turbulence [7]. For instance, Porté-Agel et al. [7] emphasized the importance of understanding wake effects and turbine spacing in wind farm design, while [8] provided insights into the impact of building geometry on wind flow dynamics around urban wind turbines. These studies, along with others by Hertwig et al. [9] and Škvorc and Kozmar [10], underscore the importance of high-resolution simulations, such as Large Eddy Simulation (LES), to capture the intricate details of wind flow in urban environments.

LES has proven to be an indispensable tool in urban wind energy research, offering the ability to resolve large-scale turbulent structures that significantly influence wind energy potential. Previous work by Blocken [11] and Bazdidi-Tehrani et al. [12] has highlighted the advantages of LES over traditional Reynolds-Averaged Navier-Stokes (RANS) models, particularly in capturing the complex interactions between urban geometry and wind flow. Additionally, advanced techniques such as Spectral Proper Orthogonal Decomposition (SPOD) have been employed to analyze wind energy potential by identifying dominant flow structures that contribute to energy production.

While it is well established in the literature that maximum wind energy typically occurs on building rooftops due to reduced turbulence and obstruction at higher elevations, this study focuses on analyzing the spatial variations of wind energy in urban environments. Specifically, we apply the SPOD technique, which has not been widely used in this context, to provide a more detailed understanding of energy flow dynamics and their correlation with urban geometry.

One of the most widely referenced studies in the validation of LES for urban wind flow is the Mock Urban Setting Test (MUST), which involved field measurements of wind speeds in a controlled urban-like environment. This large-scale field experiment has provided a robust dataset for validating CFD models, including LES. However, it is important to note that replicating the atmospheric conditions observed in MUST through LES is challenging due to the lack of control over natural wind conditions. Nonetheless, LES simulations have been used extensively to investigate the correlation of wind speeds at different heights and spatial locations within urban environments, providing valuable insights for optimizing wind energy capture.

This study aims to further explore the maximum wind energy potential in urban environments by analyzing the points that exhibit the highest correlation in wind speed. By employing LES to generate high-resolution wind speed time series, this research contributes to the growing body of knowledge on urban wind energy optimization. The findings could have significant implications for the placement and design of wind turbines in urban areas, where the interaction between wind flow and building structures presents unique challenges for energy harvesting.

## **2. Methodology**

The methodology employed in this study is divided into three key stages: CFD simulation, identification of correlated points, and estimation of maximum wind energy. Each stage plays a crucial role in achieving the study's objective of examining the maximum wind energy potential in an urban environment by analyzing points with the highest wind speed correlations.

### **2.1. CFD Simulation**

To simulate the wind flow in an urban environment, the ADREA-HF code was utilized in Efthimiou et al. [13], which is well-suited for high Reynolds number flows typical in urban settings. Given the complexity of urban airflow, where turbulence is significantly influenced by the presence of buildings and other structures, it was essential to adopt a simulation methodology capable of capturing these dynamics accurately. The LES approach was selected for this purpose due to its ability to resolve large-scale turbulent eddies while modeling smaller scales through subgrid scale models [8,9]. This method provides a detailed representation of the wind speed time series across various points within the urban landscape, which is critical for subsequent analysis.

The LES methodology simulated the wind tunnel experiment in Efthimiou et al. [13], replicating urban conditions by including detailed urban geometry and neutral atmospheric stability conditions. The simulation setup involved high-resolution grids to ensure the accuracy of the flow fields, particularly near the surfaces of buildings, where turbulence intensity is greatest [10]. The resulting wind speed data forms the foundation for the correlation and energy analyses conducted in the subsequent steps.

Previous studies have highlighted the significant influence of grid resolution on the accuracy of LES results, particularly in urban environments where turbulence is complex. Research by Blocken [11] and Bazdidi-Tehrani et al. [12] has demonstrated that finer grid resolutions lead to improved representation of small-scale turbulent eddies and flow characteristics around buildings. However, achieving high-resolution grids requires substantial computational resources, which often impose practical limitations. Despite these challenges, the chosen grid resolution in Efthimiou et al. [13] balances computational feasibility with the need for accurate flow prediction, capturing the most relevant flow structures for wind energy analysis.

It is important to acknowledge that the grid resolution selected in Efthimiou et al. [13] was a compromise between accuracy and computational feasibility. While a finer grid would undoubtedly capture more detailed turbulent structures, the resolution employed was sufficient to model large-scale wind flow dynamics. Certain small-scale features, particularly around building edges and narrow urban canyons, may not be fully resolved, which could introduce some local inaccuracies. Nonetheless, the primary goal of analyzing wind energy potential based on correlations at different points remains unaffected by these limitations.

### **2.2. Identification of correlated points**

The next step involved identifying the points within the urban environment that exhibit the highest correlation in wind speed. Cross-correlation analysis was employed

to measure the similarity between the wind speed time series at different locations as a function of the displacement of one series relative to another. This technique is vital for understanding how wind flow characteristics at one point influence or are influenced by those at another, particularly in complex urban terrains where buildings can disrupt and redirect airflow.

For each group of sensors placed at different heights within the urban canyon, cross-correlation coefficients were calculated to identify the most correlated points. These correlations were then analyzed across different heights to assess how urban geometry affects wind flow consistency. The findings from this analysis are crucial for determining the optimal placement of wind turbines or other energy-harvesting devices in urban environments, as they highlight areas where wind energy potential is maximized due to consistent wind speed patterns.

### **2.3. Estimation of maximum wind energy**

The final stage of the methodology focused on estimating the maximum wind energy at the identified correlated points. Spectral Proper Orthogonal Decomposition (SPOD) was employed for this purpose, a powerful technique used to decompose complex turbulent flow fields into orthogonal modes that capture the most energetic structures. SPOD is particularly effective in analyzing wind energy because it allows for the extraction of dominant flow features that contribute to energy production, providing a clearer understanding of where and how wind energy can be optimally harnessed.

The SPOD analysis was performed on the LES-generated wind speed time series to quantify the maximum wind energy available at different heights and locations. The results were then compared across various sensor groups to identify patterns related to urban geometry, such as the influence of building heights and spatial positioning within the urban canyon. This analysis also led to the development of an empirical equation that relates the maximum wind energy of the most correlated points to their corresponding distances, providing a practical tool for urban wind energy planning and optimization.

By combining advanced simulation techniques with robust statistical analyses, this methodology offers a comprehensive approach to understanding and optimizing wind energy potential in complex urban environments. The findings contribute to the growing body of knowledge on renewable energy integration in urban settings and offer practical insights for future energy harvesting strategies.

The calculations of wind speed correlation and maximum wind energy potential in this study are based on well-established principles in fluid dynamics and turbulence modeling. The primary method used for calculating wind speed correlations between different points in the urban environment is cross-correlation analysis. This technique provides insights into the relationship between wind speed time series from different locations, helping to identify areas where wind flow is most coherent. Cross-correlation is particularly useful in urban settings, where turbulent flow structures can significantly alter wind patterns due to the complex geometry of buildings and other obstacles.

Additionally, the energy yield calculations are grounded in the Spectral Proper Orthogonal Decomposition (SPOD) method. SPOD is a powerful statistical tool that decomposes the wind flow field into orthogonal modes, each capturing a distinct feature of the turbulent flow. By focusing on the most energetic modes, SPOD allows for the quantification of maximum wind energy at different heights and locations. This approach provides a more comprehensive understanding of how energy is distributed across the urban landscape, and it is particularly effective in identifying regions where wind energy potential is maximized.

The choice of SPOD over more traditional methods, such as the Fast Fourier Transform (FFT), lies in its ability to capture the most dominant, energy-carrying structures in turbulent flows, making it ideal for applications like urban wind energy optimization. The energy yield estimates presented in this study are, therefore, based on the contribution of these dominant modes, offering a robust framework for assessing wind energy potential in complex urban environments.

### **3. The wind tunnel experiment**

The MUST (Mock Urban Setting Test) wind tunnel experiment is a critical component in validating CFD models, particularly for urban wind flow simulations. In this experiment, obstacles were arranged in a grid pattern, simulating an urban environment with 12 rows of 10 obstacles each, where each obstacle had dimensions of 12.2 m in length, 2.42 m in width, and 2.54 m in height. The primary objective was to measure wind speeds at various points within this setup using a network of 3568 sensors, strategically placed to capture detailed wind flow data across different areas of the simulated urban environment. This data serves as a benchmark for assessing the accuracy of CFD models, including both Reynolds-Averaged Navier-Stokes (RANS) and LES methodologies, by comparing the measured wind velocities to the model predictions. The MUST experiment is renowned for its rigorous validation process and is frequently referenced in studies focused on urban wind flow dynamics.

The sensors used in the MUST wind tunnel experiment played a vital role in capturing detailed wind flow data across the simulated urban environment. A total of 3568 sensors were deployed, strategically positioned to cover various heights and locations within the test field. These sensors were arranged in different configurations, including a coarse network, a dense network, vertical profiles, and specific  $uw$  levels, to ensure comprehensive data collection. The height of the sensors ranged from 0.45 meters to 13.5 m, allowing for the measurement of wind velocity components ( $u$ ,  $v$ , and  $w$ ) at multiple levels above the ground. This extensive sensor network enabled the collection of high-resolution data, which was essential for validating the CFD models, including both RANS and LES simulations. The sensor data provided a robust dataset for comparing simulated results against experimental observations, ensuring that the models accurately reflected the complex wind dynamics present in urban environments.

### **4. The numerical simulation**

The LES approach employed in Efthimiou et al. [13] was used in this study. It is designed to capture the detailed turbulent structures in complex urban environments.

LES is a high-fidelity simulation technique that resolves the larger turbulent eddies directly while modeling the effects of the smaller scales, which are computationally expensive to simulate in full. In the context of this research, LES was applied to a computational field representing a portion of the atmospheric surface layer, using a medium-sized computational grid that accurately reflects the geometry of the urban setup. The LES simulations utilized a non-reflective boundary condition for the vertical velocity component at the outflow and a zero-gradient boundary condition for the other velocity components. Wall functions were applied to the surfaces of the buildings and the ground, with a roughness length of  $z_0 = 10\text{--}5$  m. This setup was critical for ensuring that the simulation accurately represented the flow dynamics around urban structures, providing insights into how turbulent eddies interact with the built environment. The LES results were validated against wind tunnel data from the MUST experiment in Efthimiou et al. [13], demonstrating the capability of LES to replicate the complex flow patterns observed in real-world urban settings. Full details about the numerical simulation and the wind tunnel experiment can be found in Efthimiou et al. [13]. Some details are provided in this work.

The discretization of the computational domain is presented in detail in Efthimiou et al. [13]. It is reminded that nearly 22.5 million cells are used. The selection of the grid is performed in order to be computationally manageable and near the work [14]. It is reminded that in the MUST experiment, the horizontal dimensions of the field are almost equal to 270 m, with a minimum cell size equal to 0.25 m in horizontal and vertical directions. The height of the cells near the ground satisfies the minimum grid analysis that is suggested by the work [15], i.e.,  $1/10$  of the building height (**Figure 1**). As a result, the domain among the buildings has cubic cells and then continuously expands with a factor of 1.1. In the horizontal directions, the  $dx$  and  $dy$  are kept constant (**Figure 1**) in the field of obstacles covering an area of  $172.55\text{ m} \times 198.13\text{ m}$ . Outside the obstacle area, the  $dx$  and  $dy$  extend by a factor of 1.1.

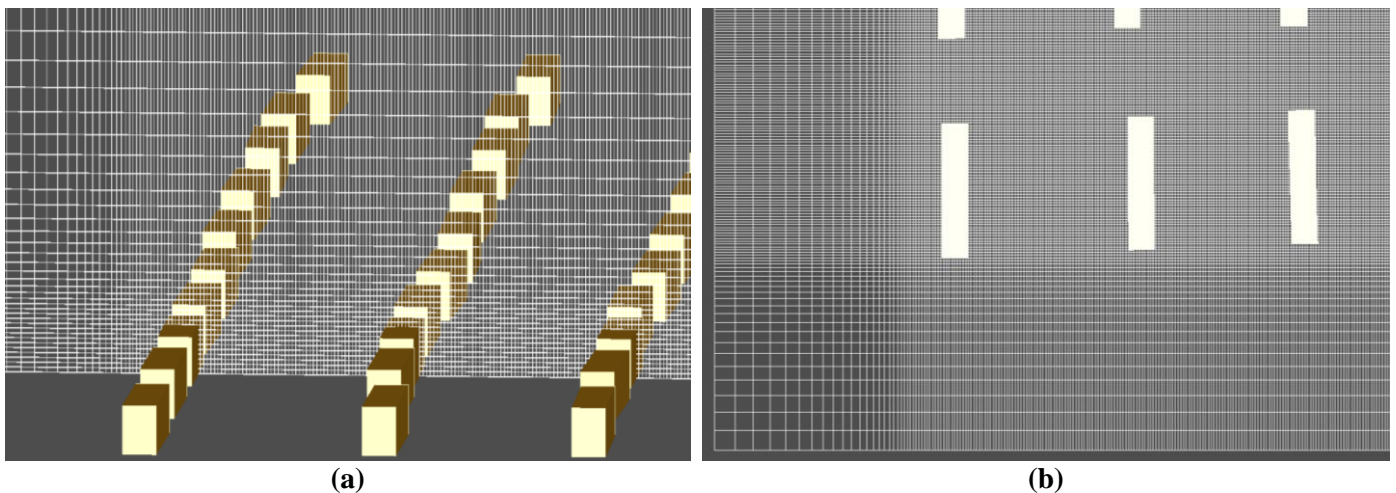


**Figure 1.** Grid details: (a) near the buildings; (b) among the buildings.

**Table 1** presents the boundary conditions for  $u$ ,  $v$  and  $w$  at each plane or solid surface of the domain. At the outlet of the flow a non-reflecting type boundary condition is used for the vertical velocity component  $u$  as well as a zero gradient boundary condition for the velocity components  $v$  and  $w$ . Rough-wall wall functions

are used at the surfaces of the buildings and the ground with a roughness length  $z_0$  equal to  $1.E-5$  m. At the inlet and at the top boundary, a zero value is set for the velocity components  $v$  and  $w$  while the Langevin boundary condition is used for the velocity component  $u$ . Concerning initial conditions, the vertical profile of the velocity component  $u$  imposed on the inlet is used throughout the field.

**Table 1.** Boundary conditions for the hydrodynamic variables ( $u, v, w$ : velocity components in the  $x-, y-, z$ -axis respectively).

Plane	Boundary condition
$-x$	Inlet: Langevin-type equation for $u, v = w = 0$
$+x$	Outlet: Non-reflecting type boundary condition for $u, \frac{\partial \varphi}{\partial x} = 0, \varphi = v, w$
$-y$	Rough-wall wall functions, roughness length = $1.0e-005$ m
$+y$	Rough-wall wall functions, roughness length = $1.0e-005$ m
Ground	Rough-wall wall functions, roughness length = $1.0e-005$ m
Top	Langevin-type equation for $u, v = w = 0$
Building walls	Rough-wall wall functions, roughness length = $1.0e-005$ m

The validation of the LES results was a crucial step in ensuring the accuracy and reliability of the simulations in replicating real-world wind flow dynamics in urban environments. This validation was conducted by comparing the LES results with experimental data obtained from the MUST wind tunnel experiment described above. Specifically, it is reminded that, in Efthimiou et al. [13], the LES-predicted velocity components ( $u, v$ , and  $w$ ) were compared against the measurements collected from a dense network of 3568 sensors strategically placed within the wind tunnel setup. The validation process utilized the hit rate (HR) metric, a quantitative measure recommended by COST Action 732 for assessing model performance. HR provides insight into the fraction of predictions that fall within an acceptable range of the measured data. The calculations took into account both the relative error and experimental uncertainty, ensuring a robust comparison. For the horizontal velocity components ( $u$  and  $v$ ), the LES model demonstrated strong performance, achieving HR values that exceed the threshold of 0.66, as outlined in COST Action 732 guidelines. Although the vertical velocity component ( $w$ ) exhibited lower HR values, this is a well-known challenge in urban wind simulations, primarily due to the complexity of vertical wind structures and the limitations of grid resolution in such environments.

The LES results showed reasonable agreement with the data, though some discrepancies were observed, likely due to the resolution limitations. This agreement provides confidence in the overall accuracy of the simulation. However, it is acknowledged that a finer grid resolution would likely improve the representation of small-scale turbulent structures, further enhancing the accuracy of localized flow predictions. Future studies will address this aspect through a detailed grid refinement study.

Although the LES model demonstrated reasonable agreement with the experimental data on a large-scale basis, it is important to note that some discrepancies may arise due to the grid resolution, particularly in regions with highly localized

turbulent structures. Nevertheless, the model captured the overall flow trends accurately, which are critical for assessing the wind energy potential in this urban configuration.

## 5. Results and discussion

### 5.1. Performance of the LES model

The performance of the LES model for each variable  $u$ ,  $v$  and  $w$  of the same experiment is presented in Efthimiou et al. [13]. In the present study the following wind speeds are validated based on the groups of the available measurements:

Coarse and fine networks:

$$U_V = \sqrt{u^2 + v^2} \quad (1)$$

$uw$  plane:

$$U_W = \sqrt{u^2 + w^2} \quad (2)$$

In **Figure 2** the quantile plots of the mean wind speeds are presented. The quantile plots are used in many scientific fields including turbulence. The results have been grouped according to the group of sensors. We observe that most of the points fall within the limits of the “1 to 2” and “2 to 1” lines for all the groups of sensors. The overall scatter of the values about the 1-to-1 line is almost similar for the coarse and fine networks and higher for the  $uw$  planes. Also, a total underprediction is obvious for all the groups of sensors and is lower for the fine network and higher for the  $uw$  plane. It should be noticed that the highest discrepancies are observed mainly for the lower values and this will be the subject of a separate study in the future by examining also their location in the domain, the wall boundary conditions and the history of turbulence.

The validation metrics (VMs) provide a quantitative way of comparing the predictions of a model with the measurements. The VMs are very useful for the validation of a model, especially in the case of a large amount of data. Various VMs are available, and each one has its advantages and disadvantages. In the present study, three VMs are used: a) The factor of two of observations within a factor of two (FAC2), the fractional bias (FB), and the normalized mean square error (NMSE). **Figure 2** presents the selected VMs for each group of sensors. It is clear that the VMs have almost their ideal values, supporting further the robustness of the LES simulation. Also, the VMs strengthen the findings of the quantile plots.

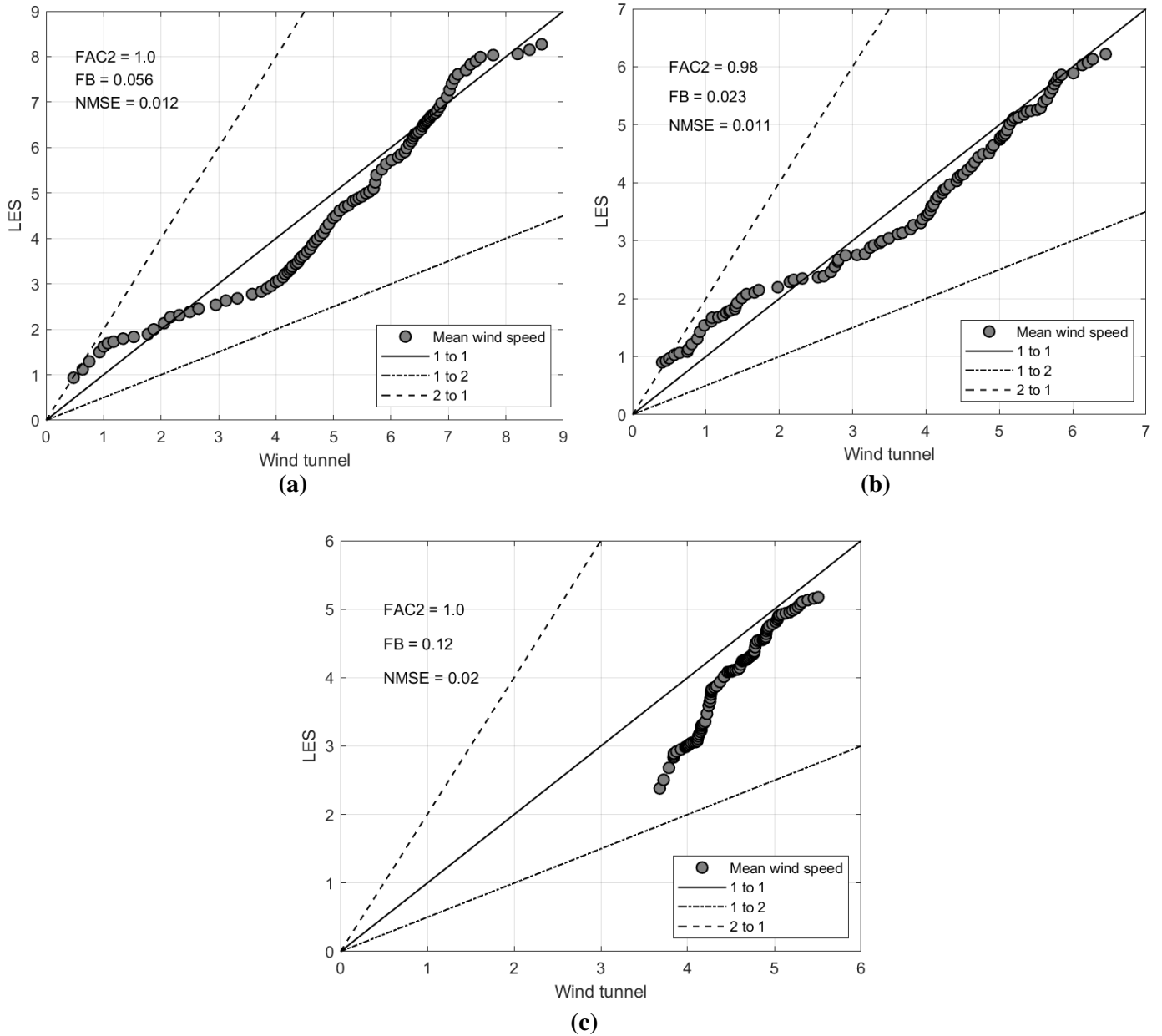


**Figure 2.** Quantile plots comparing the mean wind speeds between the wind tunnel and the LES model: (a) Coarse network; (b) Fine network; (c)  $uw$  plane. The validation metrics are also presented.

## 5.2. Maximum correlations

The statistics of the maximum correlations for each group of sensors and each height are presented in **Table 2**. It should be noticed that the autocorrelations are excluded from the analysis.

To calculate the statistics of maximum correlations, cross-correlation coefficients were employed. These coefficients quantify the similarity between two wind speed time series as a function of the displacement of one series relative to the other. The correlation coefficients in this study are computed based on the normalized cross-covariance, ensuring values fall within the range of  $-1$  to  $+1$ . Negative values indicate an inverse relationship, while positive values denote direct correlation. This approach

provides a robust framework for analyzing the influence of spatial separation and height on wind speed coherence.

The following conclusions are drawn for the statistics:

Concerning the coarse network:

- 1) There is a clear dependence on the height. The mean, maximum, and minimum values are increased with the height. On the other hand, the skewness and kurtosis are decreased with the height.
- 2) The maximum correlations are decreased as we move towards the urban area. This is due to the buildings which cause the breakup of the turbulent eddies.
- 3) The skewness is positive indicating that the tail is on the right.

Concerning the fine network:

- 4) The mean, maximum, skewness and kurtosis are close to the results of the coarse network at the height of 2.55 m.
- 5) Except for the minimum, all the other statistics of the height of 1.725 m of the fine network are close to the height of 1.28 m of the coarse network.
- 6) There is a clear dependence on the height. The mean, maximum, and minimum values are increased with the height. On the other hand, the skewness and kurtosis are decreased with the height. These are also conclusions of the coarse network.
- 7) The skewness is positive indicating that the tail is on the right.
- 8) The maximum correlations are decreased as we move deep inside the canyon. This is also the conclusion of the coarse network.

Concerning the  $uw$  plane:

- 9) The mean and kurtosis are close to the results of the coarse and fine networks at the height of 2.55 m.
- 10) The skewness is positive indicating that the tail is on the right. This is also the conclusion of the other networks.
- 11) The skewness and kurtosis have the lowest values among the corresponding ones of the other networks.

**Table 2.** Statistics of maximum correlations for each group of sensors and each height.

	Coarse network			Fine network			$uw$ plane
Height	5.1	2.55	1.28	2.55	1.725	0.9	2.55
Number of combinations	83232	92720	93330	8556	8556	8556	1482
Mean	9.75e+04	4.04e+04	1.90e+04	3.93e+04	2.41e+04	1.81e+04	3.56e+04
Maximum	1.35e+05	8.96e+04	6.99e+04	8.03e+04	7.17e+04	5.99e+04	5.75e+04
Minimum	6.54e+04	6.31e+03	9.86e+02	1.05e+04	2.19e+03	1.86e+03	1.71e+04
Skewness	0.41	0.48	0.93	0.56	0.88	1.08	0.18
Kurtosis	2.66	2.75	3.65	2.69	3.06	3.63	2.48

### 5.3. Maximum wind energy

The statistics of the maximum wind energy for each group of sensors and each height are presented in **Table 3**.

The statistics of maximum wind energy were calculated by integrating the LES-generated wind speed profiles with the empirical energy equation. The initial velocity profile at the inlet boundary was defined based on a logarithmic wind profile, while

the vertical wind speed distribution was extracted from the simulation results. This ensures that the derived wind energy values capture the spatial and height-dependent variations of wind flow in the urban environment.

The following conclusions are drawn from the statistics:

Concerning the course network:

- 12) There is again a clear dependence on the height. The mean and minimum values are increased with the height. On the other hand, the skewness is decreased with the height.
- 13) According to the mean value the maximum wind energy is decreased as we move towards the urban area. This is due to the buildings, which cause the breakup of the turbulent eddies. More specifically, this reduction in wind energy as we move deeper into the urban area can be explained by the increased interference from buildings, which causes more frequent breakup of turbulent eddies. The complex geometry of the urban environment creates areas of lower wind speeds and increased turbulence, reducing the overall available energy for capture.
- 14) The skewness is positive, indicating that the tail is on the right.
- 15) The maximum wind energy presents the highest maximum value on the roof of the buildings (2.55 m).
- 16) The maximum wind energy presents the lowest kurtosis on the roof of the buildings (2.55 m).
- 17) The minimum value of the 5.1 m presents a non-zero value in comparison with all the other cases.
- 18) The skewness and kurtosis present the highest values deep inside the canyon.

Concerning the fine network:

- 19) There is again a clear dependence on the height. The mean value is increased with the height. On the other hand, the skewness and kurtosis are decreased with the height. These are also partially conclusions of the coarse network.
- 20) The skewness is positive, indicating that the tail is on the right. This is also conclusion of the coarse network.
- 21) The skewness and kurtosis present the highest values deep inside the canyon. This is also a conclusion of the coarse network.
- 22) The maximum wind energy presents the highest maximum value deep inside the canyon.

The higher energy observed in the fine network is likely due to the increased resolution of sensors, which provides a more detailed capture of the wind flow dynamics within the urban canyon. The fine network's denser sensor placement allows for more accurate measurements of wind speed fluctuations, particularly in regions where turbulence is more pronounced, such as near building edges and narrow passageways.

The discrepancy between the mean values at 2.55 m for the coarse network (76.83) and fine network (13.01) can be attributed to differences in sensor density and spatial resolution. The coarse network provides an averaged representation of wind flow across larger grid cells, which may overestimate wind energy due to smoothing effects. In contrast, the fine network captures localized turbulence and flow structures with greater detail, leading to a more accurate but lower mean value. This highlights the critical role of resolution in urban wind energy analysis.

Concerning the  $uw$  plane:

- 23) The skewness is positive, indicating that the tail is on the right. This is also the conclusion of the other networks.
- 24) The skewness and kurtosis have the highest values among the corresponding ones of the other networks.
- 25) The maximum value is close to the corresponding value of the fine network.

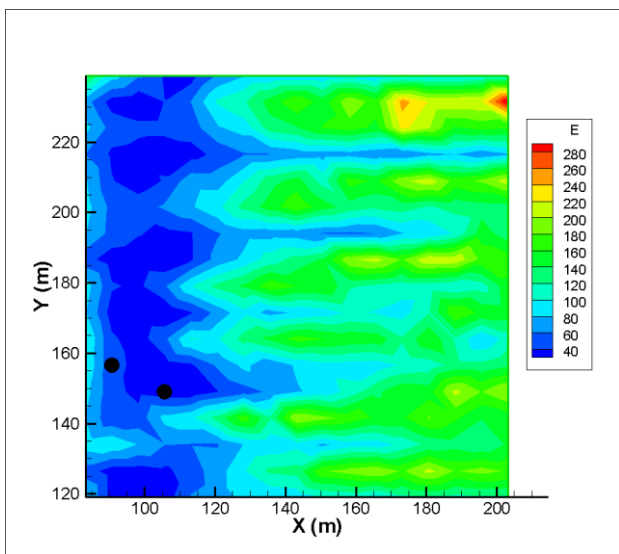
Generally, the increase in maximum wind energy with height can be attributed to the reduced impact of urban obstacles at higher elevations. As buildings and structures disrupt the wind flow more intensely at lower heights, the energy available for capture decreases. At greater heights, the wind experiences less turbulence and fewer disruptions, resulting in higher energy potential.

**Table 3.** Statistics of maximum wind energy for each group of sensors and each height.

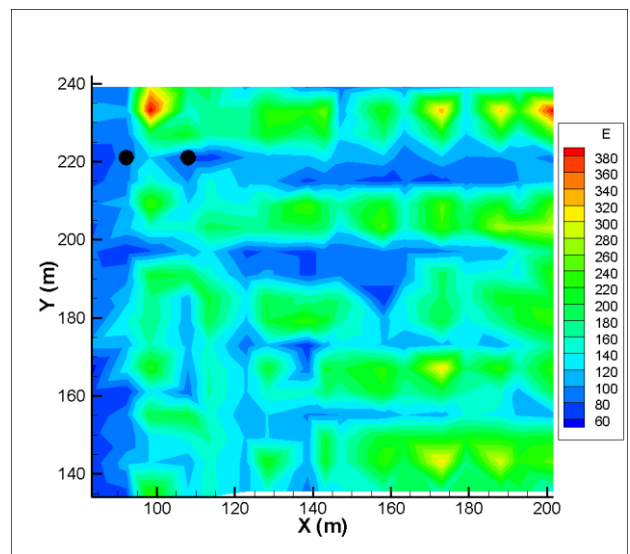
	Coarse network			Fine network			$uw$ plane
	Height	Mean	Maximum	Height	Mean	Maximum	Height
Height	5.1	2.55	1.28	2.55	1.725	0.9	2.55
Mean	104	76.83	37.06	13.01	8.43	7.54	3.75
Maximum	302	397	287	251	191	405	244
Minimum	22.28	0	0	0	0	0	0
Skewness	0.57	0.76	1.41	3.41	3.74	5.17	7.28
Kurtosis	2.77	2.69	3.93	13.81	16.54	41.72	56.32

These findings have significant implications for urban wind energy optimization. By understanding how wind energy potential varies with height and urban geometry, it is possible to identify prime locations for wind turbine placement. The higher energy at building rooftops suggests that these locations could be ideal for the installation of small wind turbines, whereas areas closer to the ground may experience lower energy yields due to increased turbulence and obstructions.

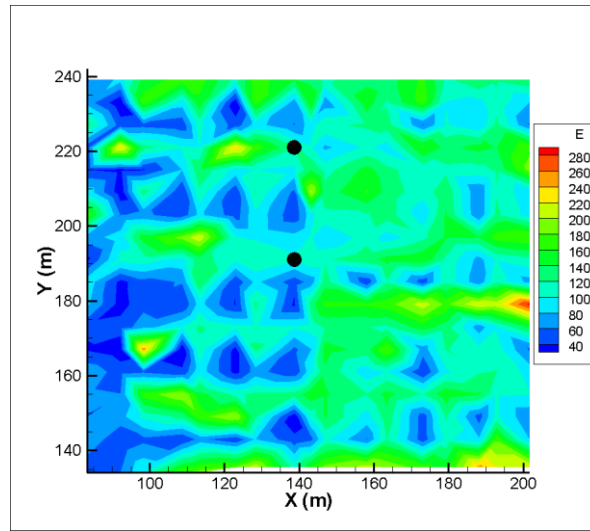
**Figures 3–5** present contour plots of the maximum wind energy for each group of sensors and height. The black circles indicate the points with the highest correlation.



(a)

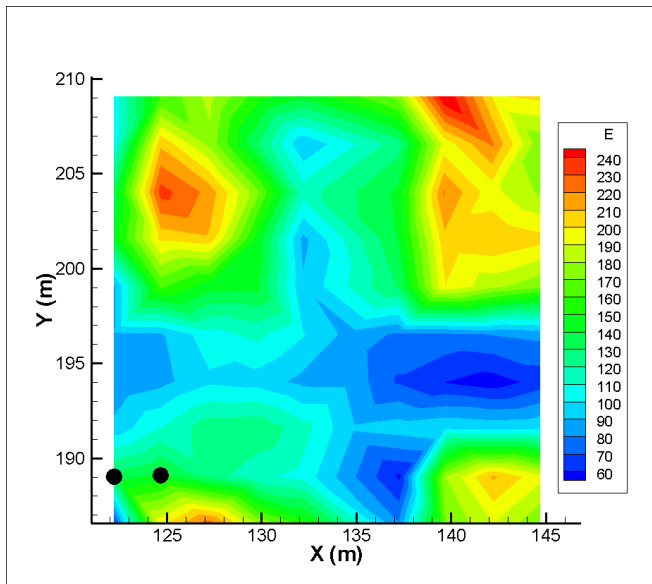


(b)

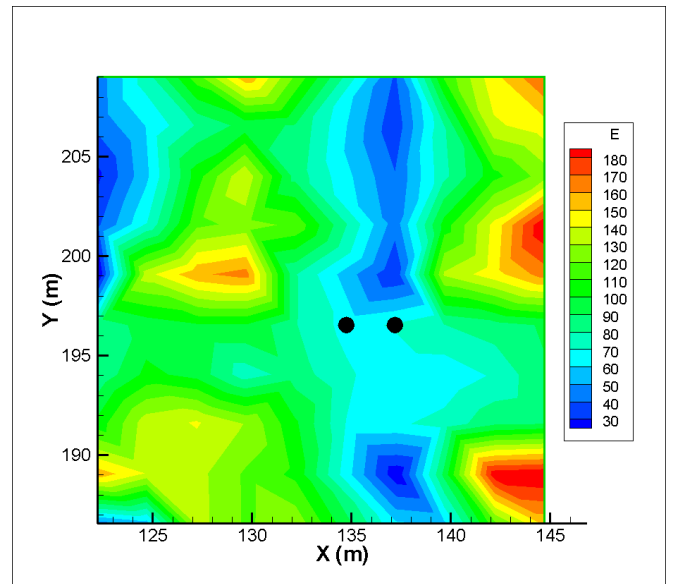


(c)

**Figure 3.** The maximum energy ( $E$  [kJ]) per group of sensors for the coarse network: (a) Height = 5.1 m; (b) Height = 2.55 m; (c) Height = 1.28 m. The black circles indicate the points with the highest correlation.



(a)



(b)

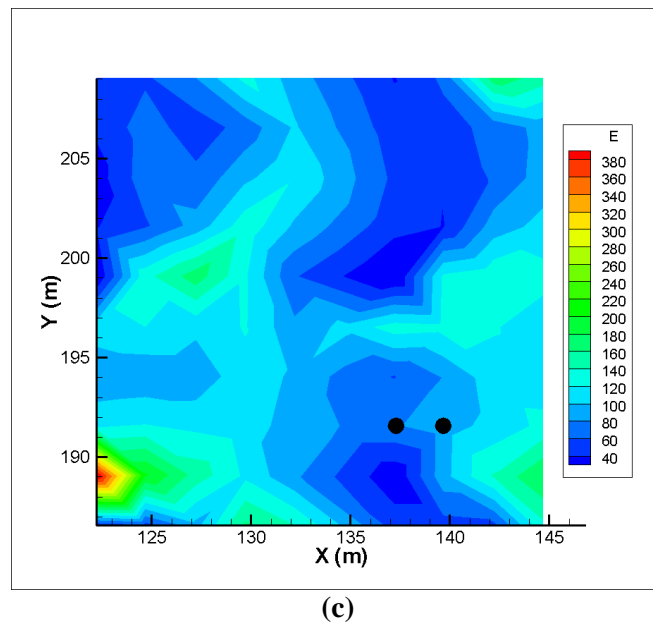


**Figure 4.** The maximum energy ( $E$  [kJ]) per group of sensors for the fine network: (a) Height = 2.55 m; (b) Height = 1.725 m; (c) Height = 0.9 m.

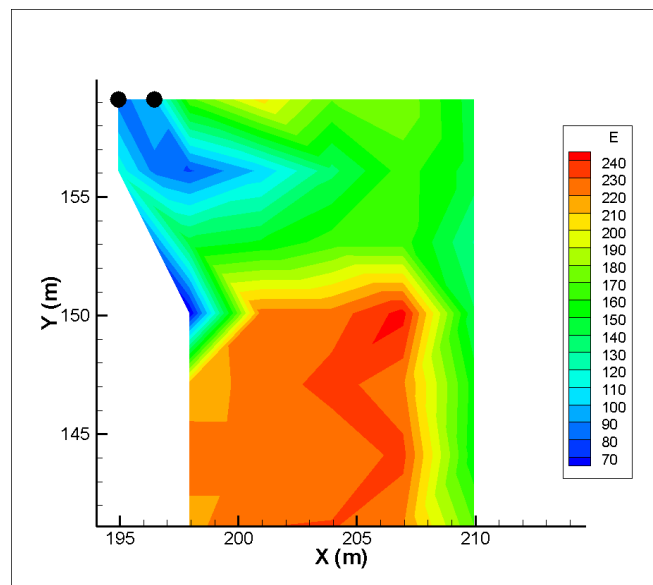


**Figure 5.** The maximum energy ( $E$  [kJ]) for the uw plane.

The figures presented in this paper depict the spatial distribution and variation of maximum wind energy potential across different sensor groups and heights within the urban canyon. Each figure provides key insights into the complex interactions between wind flow and urban geometry, helping to visualize how building structures influence the availability and intensity of wind energy.

**Figure 3** shows the maximum energy values for the coarse network across different heights. As observed, the highest energy values occur at rooftop levels (2.55 m), where the influence of building-induced turbulence is minimized, allowing for more consistent wind patterns. In contrast, energy levels decrease as we move towards

lower heights due to the increased disruption of wind flow by the surrounding structures.

**Figure 4** presents the corresponding maximum energy values for the fine network. The denser sensor placement in this network reveals a more detailed picture of wind energy distribution, particularly highlighting regions of high turbulence near building edges. The increased resolution allows for the identification of small-scale energy variations that are not apparent in the coarse network.

**Figure 5** focuses on the  $uw$  plane, illustrating the wind energy distribution across different heights. As with the other networks, the data indicates a clear increase in energy potential with height. The positive skewness observed in these figures reflects that the majority of energy values are concentrated towards the higher end of the spectrum, indicating a few locations with significantly higher energy potential.

The black circles in **Figures 3–5** indicate points of highest wind speed correlation, which are not always located in zones of maximum wind energy. This discrepancy arises due to the combined effects of spatial geometry and turbulence, where the regions of maximum wind energy may not necessarily coincide with the most coherent wind patterns. These points were selected based on their potential for stable and consistent energy yields over time.

A question that arises is if there is an equation that describes the difference of the maximum wind energy versus the distance of the most correlated points (black circles of the previous figures). **Figure 6** reveals that there is an equation with a relatively high correlation coefficient that relates the difference of the maximum wind energy of the most correlated points versus their corresponding distance. The empirical relationship illustrated in **Figure 6** is of particular interest as it demonstrates how the difference in maximum wind energy correlates with the distance between the most correlated points. This correlation supports the hypothesis that wind energy potential is highly dependent on spatial positioning within the urban environment, with points that are further apart exhibiting lower correlation and, consequently, a lower energy differential.

The empirical equation presented in **Figure 6** is derived from the analysis of wind energy data collected in this study and, to the best of the author's knowledge, has not been previously documented in the literature. This new equation offers a practical tool for predicting the difference in maximum wind energy based on the distance between the most correlated points, providing valuable insights for urban wind energy planning.

The empirical equation presented in this study is derived from the analysis of wind energy data collected at various sensor locations in the urban canyon. The equation describes the relationship between the difference in maximum wind energy and the distance between the most correlated points. This relationship was observed consistently across the data, indicating that spatial proximity plays a key role in energy distribution. Although the equation has been validated within the context of the present urban environment, further validation across different urban configurations would be valuable for assessing its broader applicability.

Future research could focus on applying this equation to a variety of urban environments to explore its robustness and generalizability. This would provide further insights into its practical utility for wind energy optimization in diverse urban settings.

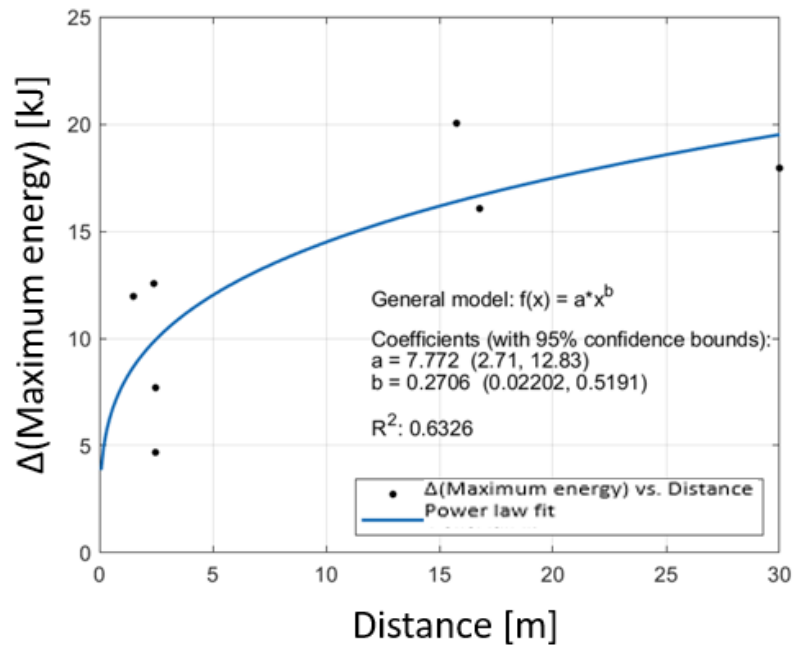


**Figure 6.** The difference of the maximum wind energy  $\Delta(\text{Maximum energy})$  versus the distance of the most correlated points.

Overall, these figures provide critical visual evidence supporting the conclusions of this study. They highlight the variability of wind energy across different heights and spatial locations, emphasizing the importance of optimizing wind turbine placement in urban environments.

The current grid resolution, while adequate for capturing the broad trends in wind energy potential, may affect the detailed representation of turbulent eddies in certain localized areas. For instance, grid refinement could lead to improved accuracy in wind speed predictions near building surfaces, which might influence the correlation patterns observed at lower heights within the urban canyon. However, the overall findings of this study, particularly regarding the identification of points with the highest wind energy potential, are expected to remain consistent. Further refinement of the grid in future studies will provide additional validation of these results.

#### 5.4. Methodological limitations

While it is acknowledged that the grid resolution employed in this study introduces certain limitations, particularly in capturing small-scale turbulent structures, the resolution used is sufficient to capture the primary flow features of interest. The chosen resolution balances computational feasibility with accuracy in predicting large-scale wind flow dynamics, which are the main focus of this study. This approach ensures that the key phenomena influencing wind energy potential in urban environments are accurately represented.

Furthermore, the resolution of the computational grid used in this study plays a critical role in the accuracy of the simulation results. It is reminded that the computational grid used in this study was meticulously designed to balance computational manageability with the need for accuracy in simulating urban wind flows. The grid encompassed a computational field with dimensions of approximately

277.85 m by 303.43 m in the horizontal directions ( $x$  and  $y$ ) and 21.06 m in the vertical direction ( $z$ ). The grid was discretized into approximately 22.5 million cells, with cell sizes ranging from a minimum of 0.25 m to a maximum of 5.14 m in the horizontal directions and from 0.25 m to 1.84 m in the vertical direction. Given the relatively low resolution employed, it is acknowledged that the errors in the present study introduced are likely to be significant. These errors primarily arise from the grid's inability to fully capture the intricate details of turbulent flow structures, especially in regions of complex geometry such as urban environments. It should be noticed that while the overall flow trends are captured, certain localized flow features, particularly near building edges and within narrow urban canyons, are less accurately represented. This limitation affects the precision of the velocity field and the correlation of wind speeds at different points, which could influence the study's conclusions regarding wind energy potential. Future work will focus on refining the grid resolution and exploring hybrid simulation techniques to mitigate these errors, ensuring more accurate and reliable predictions. Additionally, it is proposed that further studies be conducted using higher-resolution models to validate the current findings and to better understand the implications of resolution on simulation outcomes.

It is important to note that, while the LES model performs well for the horizontal components, certain discrepancies are observed in the vertical velocity ( $w$ ). These discrepancies can be attributed to the resolution of the computational grid, which may not fully capture the intricate turbulent structures present in urban canyons. Despite this, the overall performance of the LES remains reliable for the primary flow features, and the identified discrepancies do not undermine the core findings of the study. Future work may focus on further refining the grid resolution and incorporating additional experimental data to address these challenges.

Despite the acknowledged limitations related to grid resolution, the core findings of this study remain robust. The primary focus on identifying points of maximum wind energy and analyzing large-scale flow correlations is not significantly affected by the unresolved smaller-scale turbulent features. Therefore, the conclusions drawn from the analysis are reliable within the scope of this study's objectives.

## **6. Conclusions**

In this study, a comprehensive analysis of wind flow dynamics and energy potential was conducted within an urban environment using LES methodologies. The simulation of a wind tunnel experiment provided detailed wind speed time series across various spatial locations and heights, enabling a thorough investigation into the correlation patterns and energy distribution of urban wind flows.

The findings indicate a pronounced dependence of wind speed correlations on height, with higher correlations observed at increased elevations. This trend can be attributed to the diminished influence of building-induced turbulence and obstruction at greater heights, allowing for more coherent and stable wind patterns. The complex interplay between urban structures and atmospheric flow underscores the importance of considering vertical variability when assessing wind resource potential in cityscapes.

Employing the SPOD technique, the maximum wind energy was quantified across different points within the urban setting. The results reveal that building

rooftops exhibit the highest wind energy potential, highlighting these locations as prime candidates for the installation of wind energy harvesting systems. This insight is particularly valuable for urban planners and renewable energy developers aiming to optimize the integration of wind turbines in densely built environments.

Furthermore, an empirical equation was developed that relates the maximum wind energy to the distance between highly correlated points. This relationship demonstrates a significant correlation coefficient, providing a practical tool for predicting wind energy potential based on spatial parameters. Such a model can facilitate more efficient planning and deployment of wind energy infrastructure by allowing for quick assessments of prospective sites based on their spatial characteristics and proximity.

The outcomes of this research contribute to a deeper understanding of urban wind dynamics and offer actionable guidance for enhancing renewable energy utilization within cities. By identifying optimal locations and quantifying potential energy yields, this study supports the advancement of sustainable urban development and the diversification of energy sources.

Future work will focus on conducting a detailed grid refinement study to assess its impact on the accuracy of LES predictions in urban environments. Higher-resolution grids will be employed to better capture the intricate turbulent structures and wind flow patterns around buildings. Such refinements will help to further validate the correlation and wind energy findings presented here, offering a more robust foundation for optimizing wind energy potential in urban settings.

Also, for future work, it is recommended to extend this analysis by incorporating higher-resolution simulations and exploring a wider variety of urban configurations to capture an even more detailed spectrum of wind flow behaviors. Additionally, integrating real-world observational data could further validate and refine the simulation results and empirical models presented herein. Such efforts will continue to improve the accuracy and applicability of wind energy assessments in complex urban environments, fostering more resilient and sustainable urban energy systems.

Finally, future work will focus on conducting a detailed grid refinement study to assess its impact on the accuracy of LES predictions in urban environments. While the current grid resolution is sufficient for capturing the overall trends in wind energy potential, higher-resolution grids are expected to further enhance the accuracy of localized flow predictions. Such refinements will provide additional validation for the findings presented here.

**Acknowledgments:** The author would like to thank Tolia Ilias from NCSR Demokritos for performing the CFD simulation in the supercomputer ARIS (<https://hpc.grnet.gr/>).

**Institutional review board statement:** Not applicable.

**Informed consent statement:** Not applicable.

**Data availability statement:** The data that support the findings of this study are available on request from the corresponding author, GE.

**Conflict of interest:** The author declares no conflict of interest.

## References

1. Hassan Q, Viktor P, Al-Musawi TJ, et al. The renewable energy role in the global energy Transformations. *Renewable Energy Focus*. 2024; 48: 100545. doi: 10.1016/j.ref.2024.100545
2. Ishugah TF, Li Y, Wang RZ, et al. Advances in wind energy resource exploitation in urban environment: A review. *Renewable and Sustainable Energy Reviews*. 2014; 37: 613-626. doi: 10.1016/j.rser.2014.05.053
3. Stathopoulos T, Alrawashdeh H, Al-Quraan A, et al. Urban wind energy: Some views on potential and challenges. *Journal of Wind Engineering and Industrial Aerodynamics*. 2018; 179: 146-157. doi: 10.1016/j.jweia.2018.05.018
4. Fernando HJS. Fluid Dynamics of Urban Atmospheres in Complex Terrain. *Annual Review of Fluid Mechanics*. 2010; 42(1): 365-389. doi: 10.1146/annurev-fluid-121108-145459
5. Chowdhury S, Zhang J, Messac A, et al. Optimizing the arrangement and the selection of turbines for wind farms subject to varying wind conditions. *Renewable Energy*. 2013; 52: 273-282. doi: 10.1016/j.renene.2012.10.017
6. Liu YS, Yigitcanlar T, Guaralda M, et al. Leveraging the Opportunities of Wind for Cities through Urban Planning and Design: A PRISMA Review. *Sustainability*. 2022; 14(18): 11665. doi: 10.3390/su141811665
7. Porté-Agel F, Bastankhah M, Shamsoddin S. Wind-Turbine and Wind-Farm Flows: A Review. *Boundary-Layer Meteorology*. 2019; 174(1): 1-59. doi: 10.1007/s10546-019-00473-0
8. Toja-Silva F, Kono T, Peralta C, et al. A review of computational fluid dynamics (CFD) simulations of the wind flow around buildings for urban wind energy exploitation. *Journal of Wind Engineering and Industrial Aerodynamics*. 2018; 180: 66-87. doi: 10.1016/j.jweia.2018.07.010
9. Hertwig D, Patnaik G, Leitl B. LES validation of urban flow, part I: flow statistics and frequency distributions. *Environmental Fluid Mechanics*. 2016; 17(3): 521-550. doi: 10.1007/s10652-016-9507-7
10. Škvorec P, Kozmar H. Wind energy harnessing on tall buildings in urban environments. *Renewable and Sustainable Energy Reviews*. 2021; 152: 111662. doi: 10.1016/j.rser.2021.111662
11. Blocken B. Computational Fluid Dynamics for urban physics: Importance, scales, possibilities, limitations and ten tips and tricks towards accurate and reliable simulations. *Building and Environment*. 2015; 91: 219-245. doi: 10.1016/j.buildenv.2015.02.015
12. Bazdidi-Tehrani F, Ghafouri A, Jadidi M. Grid resolution assessment in large eddy simulation of dispersion around an isolated cubic building. *Journal of Wind Engineering and Industrial Aerodynamics*. 2013; 121: 1-15. doi: 10.1016/j.jweia.2013.07.003
13. Efthimiou G, Barmpas F, Tsegas G, et al. Development of an Algorithm for Prediction of the Wind Speed in Renewable Energy Environments. *Fluids*. 2021; 6(12): 461. doi: 10.3390/fluids6120461
14. Efthimiou GC. Prediction of four concentration moments of an airborne material released from a point source in an urban environment. *Journal of Wind Engineering and Industrial Aerodynamics*. 2019; 184: 247-255. doi: 10.1016/j.jweia.2018.11.032
15. Tominaga Y, Mochida A, Yoshie R, et al. AIJ guidelines for practical applications of CFD to pedestrian wind environment around buildings. *Journal of Wind Engineering and Industrial Aerodynamics*. 2008; 96(10-11): 1749-1761. doi: 10.1016/j.jweia.2008.02.058